Membrane Currents in Retinal Bipolar Cells of the Axolotl

MARC TESSIER-LAVIGNE, DAVID ATTWELL, PETER MOBBS, and MARTIN WILSON

From the Department of Physiology, University College London, London WC1E 6BT, England, and the Department of Zoology, University of California, Davis, California 95616

ABSTRACT By whole-cell patch-clamping bipolar cells isolated from enzymatically dissociated retinae, we have studied the nonsynaptic ionic currents that may play a role in shaping the bipolar cell light response and in determining the level of voltage noise in these cells. Between −30 and −70 mV, the membrane current of isolated bipolar cells is time independent, and the input resistance is 1–2 GΩ. Depolarization past −30 mV activates an outward current (in <100 ms), which then inactivates slowly (~1 s). Inactivation of this current is removed by hyperpolarization over the range −20 to −80 mV. This current is carried largely by K ions. It is not activated by internal Ca^{2+}. The membrane current of isolated bipolar cells is noisy, and the variance of this noise has a minimum between −40 and −60 mV. At its minimum, the standard deviation of the voltage noise produced by nonsynaptic membrane currents is at least 100 μV. The membrane currents of depolarizing bipolar cells in slices of retina were investigated by whole-cell patch-clamping. Their membrane properties were similar to those of isolated bipolar cells, but with a larger membrane capacitance and a smaller input resistance. Their membrane current noise also showed a minimum near −40 to −60 mV. The time-dependent potassium current in axolotl bipolar cells is not significantly activated in the physiological potential range and can therefore play little role in shaping the bipolar cells' voltage response to light. Differences in the waveform of the light response of bipolar cells and photoreceptors must be ascribed to shaping by the synapses between these cells. The noise minimum in the bipolar membrane current is near the dark potential of these cells, and this may be advantageous for the detection of weak signals by the bipolar cells.

INTRODUCTION

Retinal bipolar cells are the second neuron layer in the visual system and are the main link between the inner and outer retina. Their receptive field has a center-surround organization. When light falls on the receptive field center, the resulting hyperpolarization of photoreceptors decreases neurotransmitter release at

Address reprint requests to Dr. Martin Wilson, Dept. of Zoology, University of California, Davis, CA 95616.

J. GEN. PHYSIOL. © The Rockefeller University Press · 0022-1295/88/01/0049/24$2.00

Volume 91 January 1988 49–72

the photoreceptor–bipolar cell synapse and produces a graded voltage change in the bipolar cell. Light falling in the receptive field surround produces a potential change of the opposite sign, mediated either through a direct synaptic input from horizontal cells to bipolar cells or by a feedback synapse from horizontal cells to cones. Bipolar cells fall into two classes defined by their voltage response to central light: depolarizing and hyperpolarizing.

An examination of the membrane currents of bipolar cells may help our understanding of several fundamental mechanisms by which the retina processes information. Since the voltage response of bipolar cells to light is more transient than that of photoreceptors (Schwartz, 1974; Ashmore and Falk, 1980; Ashmore and Copenhagen, 1980), it is possible that voltage-gated currents in bipolar cells play an important role in signal shaping. Such shaping is known to occur in rods and to a lesser extent in cones: voltage-gated currents make the voltage response to light more transient than the waveform of the current change evoked by light in the receptor outer segments (Detwiler et al., 1978; Attwell and Wilson, 1980; Attwell et al., 1982; Baylor et al., 1984; Baylor and Nunn, 1986). Bipolar cells represent the first place in the visual system where information is separated into different channels: depolarizing bipolar cells make contact with "on" ganglion cells, and hyperpolarizing bipolar cells make contact with "off" ganglion cells (Miller and Dacheux, 1976). It is important to know how bipolar cells in these two separate pathways differ in their properties, and to what extent bipolar cell membrane currents contribute to the overall performance of these different information channels. Finally, the ability of the retina to detect dim stimuli implies that the voltage noise caused by the random opening and closing of ion channels in the bipolar cell membrane must be relatively small (Falk and Fatt, 1974).

In this article, we examine the membrane properties of axolotl bipolar cells to understand how currents intrinsic to these cells' membranes shape the bipolar light response and to what extent the noise contributed by these intrinsic currents limits the ability of the bipolar cells to detect dim stimuli. The majority of our experiments were carried out on bipolar cells isolated from enzymatically dissociated retinae, in order to avoid complications of interpretation arising from the synaptic input from other retinal cells. We also performed some experiments on bipolar cells in living slices of retina. We voltage-clamped cells to study their membrane currents, using the whole-cell variant of the patch-clamp technique (Hamill et al., 1981). The results differ in important ways from those obtained by Kaneko and Tachibana (1985) for goldfish bipolar cells and suggest that signal processing by bipolar cells of these two species is quite dissimilar.

Some preliminary reports on part of these studies have been published (Attwell et al., 1985*a*, *b*, 1986).

METHODS

Experiments were carried out on retinae from larval axolotls, *Ambystoma mexicanum*.

Isolated Bipolar Cells

Isolated bipolar cells were obtained by papain dissociation of the retina, using the method of Bader et al. (1979). Bipolar cells were identified by their characteristic shape, with a

Landolt club (Landolt, 1871; Cajal, 1893; Lasansky, 1973) at one end of the soma and an axon at the other end. Dendrites were often seen at the Landolt-club end of the cell. Membrane currents were not significantly different in cells that possessed or lacked dendrites. The results reported here were obtained by patch-clamping >500 isolated bipolar cells. Unless otherwise stated, each result was obtained in at least six different cells.

Bipolar Cells in Retinal Slices

Retinal slices (Werblin, 1978) were used to study the properties of bipolar cells in the retina. Since this preparation exposes the cell bodies of all retinal cell types, patch recording electrodes can be moved up to a cell's membrane surface for gigaseal formation. Experiments were performed using infrared illumination and an image converter in order to preserve the cells' light responses.

Identification of bipolar cells was based on their position in the retina, on their light response, and sometimes on subsequent observation of the cell's morphology using fluorescence microscopy: the fluorescent dye Lucifer yellow was included in the patch recording electrode (1 mg/ml) and entered the cell after rupture of the membrane patch when passing to the whole-cell clamp mode.

TABLE I

External Solutions

	Normal solution	High K			Zero Ca
		mM			
NaCl	88	74.5	39.5	—	88
KCl	1.5	15	50	89.5	1.5
$CaCl_2$	3	3	3	3	—
$MgCl_2$	0.5	0.5	0.5	0.5	3.5
EGTA	—	—	—	—	0.2

External solutions contained (in millimolar): 15 glucose, 20 HEPES, 0.5 $NaHCO_3$, 1 NaH_2PO_4, 1 Na-pyruvate.
The pH was adjusted to 7.25 with ~8 mM NaOH.

Solutions

The external solution used to superfuse the cells and the various solutions used to fill the patch pipettes are given in Tables I and II. Table II includes the free Ca^{2+} concentrations calculated for the patch pipette solutions (see p. 64) using the equilibrium constant for Ca^{2+} binding to EGTA and the CaF_2 solubility given in Smith and Martell (1976).

Small ions in the patch pipette solution replace those of the cell cytoplasm within 30–60 s of transition to the whole-cell recording mode (Fenwick et al., 1982). We have therefore been able to study the effect of different internal K^+ and Cl^- concentrations and different internal Ca^{2+} concentrations and Ca^{2+} buffering strengths by using the different pipette solutions shown in Table II.

Patch Electrodes, Series Resistance, Cell Capacitance, and Tip Potentials

Recordings were made using a patch-clamp (EPC-5 or EPC-7, List-Medical, Darmstadt, Federal Republic of Germany). The electrodes used had resistances in the range 3–10 MΩ before a seal was formed. Cell-attached seal resistances of >20 GΩ were sometimes obtained, but typical values were in the range 1–10 GΩ. The membrane capacitance, C,

and series resistance at the mouth of the patch pipette, R_p, were measured from the current response to a small voltage-clamp step applied from a holding potential of −50 mV. In this potential range, there is no contribution of voltage-gated currents to the membrane current (see below), and the cell can be treated as the parallel combination of a capacitor, C, and a resistor, R_{in}, which includes the parallel shunt of the seal resistance between the cell and the electrode (see inset to Fig. 2). The current flow predicted from the model circuit, shown in the inset to Fig. 1 *A*, has the waveform

$$\Delta I(t) = \frac{\Delta V}{R_{in} + R_p}\left(1 + \frac{R_{in}e^{-t/\tau}}{R_p}\right), \quad (1)$$

where t is the time after application of the voltage-clamp step, $\tau = CR_{in}R_p/(R_{in} + R_p)$, and ΔV is amplitude of the voltage-clamp step applied. Thus, the current amplitude at $t = 0$

TABLE II

Internal Solutions

	A 100 $[Cl]_i$	B 30 $[Cl]_i$	C 30 $[Cl]_i$ + ATP	D 10 $[Cl]_i$	E Low EGTA	F High EGTA	G KF	H Cs	I Choline
KCl	100	30	30	10	30	16.5	—	—	—
K-acetate	—	70	70	90	70	70	—	—	—
EGTA	0.6	0.6	0.6	0.6	0.02	5	5	5	5
$MnCl_2$*	—	—	—	—	—	0.5	0.5	0.5	0.5
$MgCl_2$	—	—	2	—	—	—	—	—	—
ATP	—	—	1	—	—	—	—	—	—
KF	—	—	—	—	—	—	86.5	—	—
CsCl	—	—	—	—	—	—	—	92.5	—
Choline Cl	—	—	—	—	—	—	—	—	92.5
NaCl	—	—	—	—	—	6	6	—	—
NaOH	5.4	4.4	6.0	4.4	3.0	—	—	16.2	16.2
KOH	—	—	—	—	—	16.2	16.2	—	—
Calculated free $[Ca^{2+}]$	11.3 nM	11.3 nM	11.9 nM	11.3 nM	1.5 μM	42 nM	<5.2 nM	42 nM	42 nM
Tip potential (*mV*)	−2.5	−5.8	−5.8	−7	−5	−5.8	−3.5	−3.3	−0.2

Internal solutions contained 13.3 mM HEPES.

The pH was adjusted to 7.0 with NaOH or KOH as listed. Concentrations are in millimolar unless otherwise indicated.

* Measurements with a Ca^{2+}-sensitive electrode showed that, in the absence of added Ca^{2+}, the concentration of Ca^{2+} contributed as an impurity in other reagents was 17.5 μM.

(obtained by semilogarithmic extrapolation) is $\Delta I(0) = \Delta V/R_p$, which allows us to calculate R_p. The steady state current is $\Delta I(\infty) = \Delta V/(R_{in} + R_p)$, which allows us to calculate R_{in}. The membrane capacitance can then be calculated from the time constant of the current relaxation as $C = \tau(R_{in} + R_p)/(R_{in}R_p)$. This reduces to the more commonly quoted $C = \tau/R_p$ (Marty and Neher, 1983) if the cell input resistance is infinitely greater than the pipette resistance. For bipolar cells in retinal slices, which have a relatively low resistance (as described later), it was essential to use the full expression for the capacitance. Fig. 1 shows an example of a capacity transient used for these calculations. The semilogarithmic plot of the decay of the transient is linear, consistent with our treatment of the cell as a lumped resistor and capacitance.

In whole-cell mode, the pipette resistance, R_p, was in the range 4–60 MΩ. The voltage error (pipette resistance × current flowing) produced by the pipette resistance was

corrected for by subtraction from the nominal voltage-clamp potential (although data were discarded if the product of the pipette resistance and any time-dependent change in current during a voltage-clamp pulse was >5 mV). Data for noise analysis were discarded if filtering by the pipette series resistance [half-power frequency $1/(2\pi\tau)$, typically 500–2,000 Hz] was significant in the frequency range of interest.

Tip potentials were corrected for as described by Fenwick et al. (1982). The tip potentials measured in normal external solution for the different internal solutions used are given in Table II.

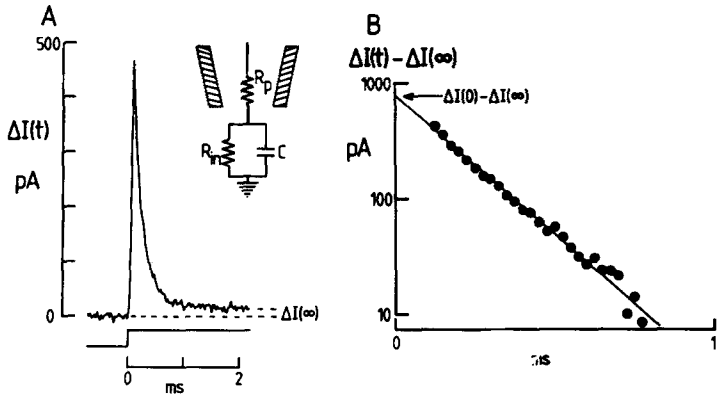

FIGURE 1. Analysis of cell capacitance, C, and pipette series resistance, R_p. (*A*) Current flow in response to a 10-mV depolarization (bottom trace) from a holding potential of −50 mV. The inset shows the circuit used for analysis of the capacity transient. R_{in} represents the parallel combination of the cell resistance and the resistance of the seal between the electrode and the cell (see inset to Fig. 2: the "battery" representing the resting potential of the cell is omitted for simplicity). Unlike for other records shown in this article, no electronic subtraction of the capacity current has been applied. The current does not rise instantaneously at $t = 0$, as in Eq. 1, because of filtering by the tape recorder. (*B*) Semilogarithmic plot of the decay of current in *A* to its steady value, $I(\infty)$. The plot is a reasonable exponential over approximately four time constants ($\tau = 0.18$ ms). For this cell, the series resistance (calculated as described in the text) was 12.6 MΩ, the capacitance was 14.6 pF, and the cell input resistance was 670 MΩ.

RESULTS

The results are presented in three sections. First, the membrane currents of isolated bipolar cells in normal solution are described. These data allow us to assess the contribution of the currents to shaping of the light response and to voltage noise in the cell. Second, we report ion-substitution experiments investigating further the membrane currents in these cells. Third, the properties of bipolar cells in retinal slices are described. These experiments form an important control, to check that the properties of bipolar cells are not grossly altered by enzymatic isolation from the retina.

Membrane Currents of Isolated Bipolar Cells

Resting potentials. We considered it possible that, in the absence of synaptic input from photoreceptors and other retinal neurons, the resting potentials of

isolated depolarizing and hyperpolarizing bipolar cells might be different. For example, if one considered only the photoreceptor input to bipolar cells, removal of that input by cell isolation would result in depolarizing bipolar cells having a more positive resting potential than hyperpolarizing bipolar cells. Removal of other synaptic inputs (for example, from horizontal and amacrine cells) may tend to blur this distinction. To test whether isolated bipolar cells could be identified simply on the basis of resting potential, we investigated whether their resting potentials fell into two distinct classes.

Fig. 2 shows a histogram of resting potentials obtained in 62 cells when the patch pipette was filled with a pseudo-intracellular medium containing 30 mM Cl^- (solution B or C in Table II: the resting potential and membrane currents

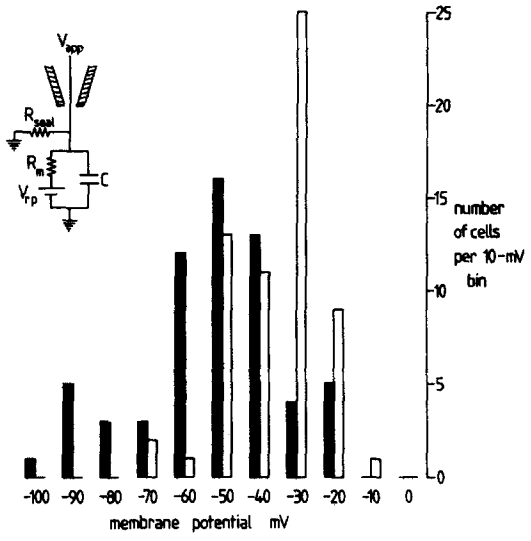

FIGURE 2. Histograms of the distribution of resting potentials found in 62 isolated bipolar cells, with solution B or C from Table II (30 mM $[Cl^-]$) in the patch pipette. The open columns are the distribution found for the resting potential, defined as the pipette potential at which no current flowed through the patch pipette. The mean resting potential was −35 mV. The filled columns are the distribution obtained after correcting for the non-infinite seal resistance by Eq. 2. The mean resting potential was −53 mV. The inset shows the model circuit used to derive Eq. 2. R_m and C denote the cell membrane resistance and capacitance. V_{rp} is the apparent resting potential in the presence of shunting by the seal made between the cell membrane and the patch pipette.

were not significantly different when ATP was included in [solution C] or omitted from [solution B] the pipette). We used 30 mM $[Cl^-]$ solutions as our standard internal medium for most experiments. The resting potential was determined as the pipette potential for which no pipette current flowed in the whole-cell clamp mode (measured ~1 min after passing to the whole-cell mode, i.e., after equilibration of the cell contents with the ions in the patch pipette, but before washout of larger intracellular molecules). This produced an approximately unimodal histogram, with a mean value of −35 ± 12 mV (SD).

The wide range of resting potentials encountered was surprising; we therefore investigated whether this was a result of variability in the resistance of the seal between the patch pipette and the cell membrane, R_{seal}. The input resistance of isolated bipolar cells (R_{in} ~ 1.3 GΩ; see below) was often comparable to R_{seal} (1–

20 GΩ, measured in the cell-attached configuration before a whole-cell clamp was obtained, and thus ignoring the conductance of the patch of membrane under the electrode). It is likely, therefore, that the apparent resting potential, V_{app}, is reduced from the true value, V_{rp}, by the shunt through the seal resistance. To analyze this, we treated the seal resistance as a nonselective leak to earth (with a reversal potential of zero), which is assumed not to be altered during the rupturing of the membrane patch to obtain a whole-cell clamp (see the equivalent circuit in the inset to Fig. 2). On this basis, the relationship between the apparent and true resting potential is

$$V_{rp}/V_{app} = R_{seal}/(R_{seal} - R_{in}), \quad (2)$$

and the input resistance is related to the true membrane resistance, R_m, by

$$1/R_{in} = 1/R_m + 1/R_{seal}. \quad (3)$$

Correcting each resting potential for the seal resistance of the pipette used to record it altered the mean resting potential to −53 ± 19 mV, but the corrected resting potential histogram was still roughly unimodal (Fig. 2).

The histograms in Fig. 2 do not allow us to divide our (morphologically indistinguishable) isolated bipolar cells into clearly distinct classes on the basis of resting potential. However, the fact that different bipolar cells can exhibit either an inward current or an outward current in response to glutamate, the putative photoreceptor transmitter, suggests that both depolarizing and hyperpolarizing bipolar cells are obtained by the isolation procedure (Attwell et al., 1987).

Capacitance. In 174 cells, the mean capacitance, measured as described in the Methods, was 11.4 ± 4.5 pF. To estimate the capacitance per unit area of membrane for nine cells, the surface membrane area was estimated from video recordings of the cells' image, after measuring the cells' capacitance. The mean specific capacitance was 1.49 ± 0.36 $\mu F/cm^2$. The presence of any surface infoldings not visible from the video image would lead to this being an overestimate.

Ionic currents in normal external solution and 30 mM [Cl^-] internal solution. Fig. 3 shows typical voltage-clamped currents obtained on stepping the potential from a holding level of −58 mV to various other potentials. These data were obtained with a patch pipette filled with a solution containing 30 mM [Cl^-] (solution C in Table II). At potentials more negative than −30 mV, the ionic current was time independent and roughly ohmic. The mean input resistance at −50 mV was 1.3 ± 2.2 GΩ (n = 106 cells). Correction for the seal conductance using Eq. 3 gave an estimate for the cell resistance of 2.04 ± 0.57 GΩ (n = 66).

Time-dependent currents activated by depolarization. Depolarization to potentials more positive than −30 mV produced a rapid, time-dependent increase of outward current (Fig. 3*A*), which then decreased again more slowly (Fig. 3*B*). The kinetics of the current increase and decrease varied significantly between cells, but tended to be faster for pulses to more positive potentials. The slow decrease in current was not exponential and occasionally showed two distinct phases: a fast sag, followed by a slower sag. The decrease in current makes the peak current-voltage relation of the cell (at early times after a voltage-clamp step)

show much more outward rectification than the steady state current-voltage relation (Fig. 3*C*).

The experiments described below show that the time-dependent outward current is carried largely by K ions and has a reversal potential between −60 and −90 mV. We therefore attribute the time course of the current change at

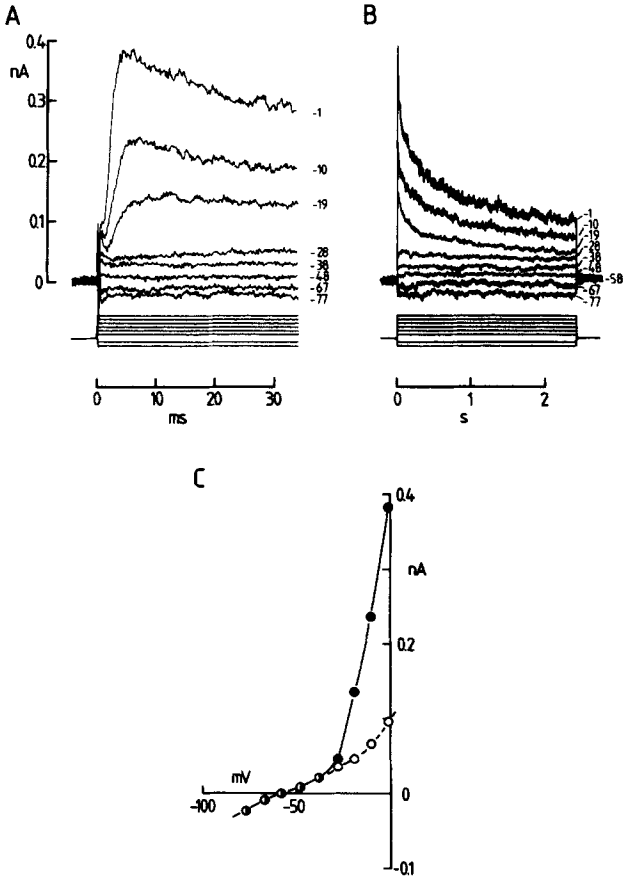

FIGURE 3. Ionic currents in the bipolar cell membrane in normal external solution and with 30 mM [Cl^-] (solution C of Table II) in the patch pipette. (*A* and *B*) The cell was voltage-clamped to different potentials (shown by each trace) from a holding potential of −58 mV. Responses are shown on a fast time base in *A* and on a slower time base in *B*. The biphasic current change, seen in *A* as a fast transient in the first 0.5 ms after changing the voltage and as a slower sag in the current extending to 1.5 ms (particularly clear in the records for −77 and −19 mV), is due to imperfect electronic subtraction of the current charging the capacitance of the cell and patch pipette. Depolarization past −30 mV produces a rapid increase (*A*) followed by a slow decrease (*B*) in outward current. (*C*) Current-voltage relations measured at the peak (filled circles) of the outward current in *A*, and at the end of the pulses in *B* (open circles), when the current is almost at its steady state value at each potential. The slope resistance was 1.05 GΩ near −60 mV and 70 MΩ near 0 mV for the peak current-voltage curve.

depolarized potentials to fast activation (Fig. 3*A*), followed by slow inactivation (Fig. 3*B*) of an outward current. This account is similar to that given previously for the qualitatively similar K^+ currents seen in molluscan neurons and T lymphocytes (Connor and Stevens, 1971*a*, *b*; Aldrich et al., 1979; Fukushima et al., 1984; Cahalan et al., 1985).

The time-dependent currents shown in Fig. 3 were seen in 90% of the cells studied (irrespective of whether cells showed an inward or an outward current at −50 mV in response to glutamate, identifying them as presumed hyperpolarizing and depolarizing cells, respectively; Attwell et al., 1987). 10% of the cells, however, showed very little time-dependent current, although their membrane current-voltage relation showed some outward rectification, as for the steady state curve in Fig. 3. We are uncertain whether these cells form a functionally distinct class of bipolar cells in the retina, or whether they were simply damaged during the isolation or recording procedure in such a way as to alter their membrane currents while leaving them as viable cells.

Current tails seen after depolarizing pulses. On repolarizing to the holding potential after evoking the time-dependent current by depolarization in Fig. 3, little or no time-dependent current tail was seen. This absence of a large current tail comes about because, as we now show, the holding potential is near the reversal potential for the time-dependent current evoked by depolarization and much of the outward current is inactivated after the long pulse in Fig. 3.

Fig. 4 shows an experiment in which the cell was repolarized to the holding potential before much inactivation had occurred. After depolarizing from −59 to 0 mV in order to activate the outward current, the cell was repolarized to different "post-pulse" potentials, to reveal current tails reflecting the reversal of gating changes occurring during the depolarizing step. Since relatively little inactivation occurs during the main pulse and the inactivation kinetics are an order of magnitude slower than the activation kinetics (Fig. 3), the tails seen reflect mainly the removal of activation of the current on hyperpolarizing. For post-pulse potentials more positive than −60 mV, a decaying outward current tail was seen. At −69 mV the tail was flat, and negative to −70 mV a decaying inward tail was observed. In seven cells, the average reversal potential obtained was −77 ± 9 mV, which suggests that the time-dependent current is carried largely, but not entirely, by K ions. (The Nernst potentials for K^+, Cl^-, and Na^+ are −105, −29, and +70 mV, respectively, for solution C of Table II in the patch pipette and hence in the cell.) If the only other ion carrying this current is Na, one can calculate from the Goldman (1943) equation that the permeability of the channels to Na ions is only 0.033 times the permeability to K ions. Similarly, if the current is carried partly by Cl ions, then $P_{Cl}/P_K = 0.13$. Experiments in which the external or internal K^+ concentration was changed (described below) reinforced the conclusion that the time-dependent current is carried mainly by K ions.

Activation and inactivation curves for the gated current. Fig. 5*B* shows typical data for the voltage dependence of activation of the time-dependent conductance (dashed curve). To obtain this, the peak time-dependent outward current was divided by $(V - V_{rev})$, where V_{rev} is the reversal potential obtained in experiments

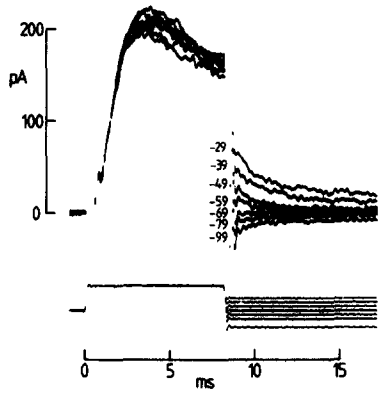

FIGURE 4. Reversal potential of the time-dependent current activated by depolarization. Current is shown as the top trace; voltage is shown as the bottom trace. A bipolar cell was briefly depolarized from a holding potential of −59 to 0 mV to activate the time-dependent outward current. Then, before much inactivation of the outward current had occurred, the potential was changed to one of various post-pulse potentials (shown by each trace). The current tail, representing the deactivation of the time-dependent current, reversed at around −69 mV. The capacity current is largely off-screen. Small oscillations in voltage and current after a voltage change are produced by a filter in the tape recorder and do not occur in the cell. Solution B of Table II was in the patch pipette.

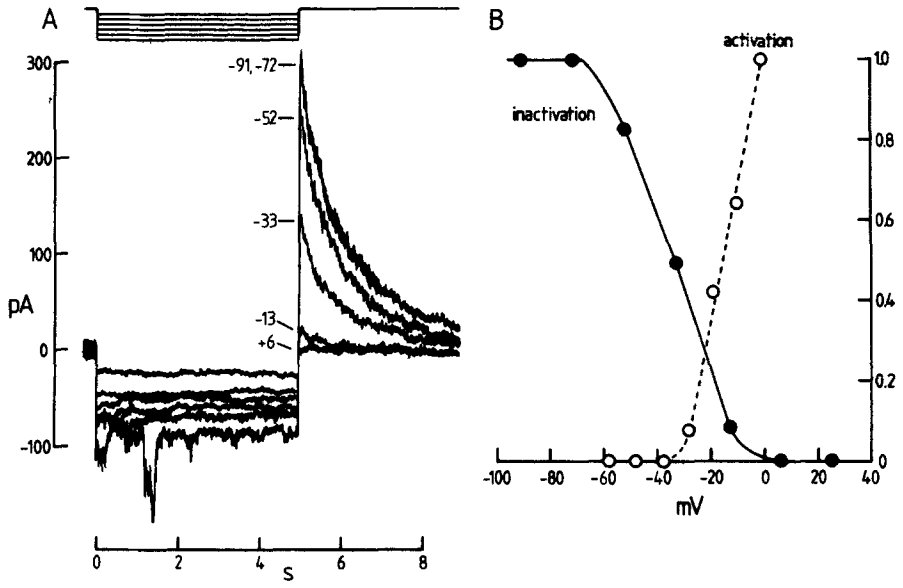

FIGURE 5. Activation and inactivation curves for the time-dependent outward current. (*A*) Data for the inactivation curve. Currents were evoked on hyperpolarizing the cell to various potentials from a holding potential of +25 mV and then returned to +25 mV. The pulse potential is shown by each current overshoot seen on returning to +25 mV. The overshoots after pulses to −72 and −91 mV superimpose. During the hyperpolarization to −92 mV, large step-like noise events are seen. Solution F of Table II was in the patch pipette. (*B*) The filled symbols show a plot of the amplitude of the current overshoots seen at +25 mV in *A*, as a function of pulse potential, normalized to the overshoot evoked by large hyperpolarizing pulses. The open symbols show the voltage dependence of the peak time-dependent conductance for the cell of Fig. 3, derived as described in the text, and normalized to the conductance evoked by the largest depolarization applied.

like that of Fig. 4 (Hodgkin and Huxley, 1952*a*). The peak conductance derived in this way increases with depolarization above −30 mV and does not saturate by 0 mV.

Fig. 5*A* shows an experiment designed to reveal how inactivation of the time-dependent current depends on membrane potential. Hyperpolarizing pulses of various amplitudes were applied from a holding potential of +25 mV. During the pulse, inactivation of the gated current was removed so that, on repolarization to +25 mV, a large outward current was activated (followed by a sag back to the original current level as the gated current inactivated again). If activation of the current occurs sufficiently quickly when the membrane potential is returned to +25 mV, the peak outward current amplitude evoked at this time reflects the amount of inactivation removed by the hyperpolarizing pulse (Hodgkin and Huxley, 1952*b*). In Fig. 5*B*, this current amplitude is plotted as a function of pulse potential, normalized to the amplitude produced by large hyperpolarizing pulses.

These data show that, over the physiological potential range, inactivation of the gated current is removed by hyperpolarization. Below −70 mV, no further inactivation is removed by hyperpolarization, and at potentials positive to 0 mV, the current is completely inactivated in the steady state. Using hyperpolarizing pulses of various durations, we found that inactivation was removed with a roughly exponential time course, with a time constant of ~1 s at −80 mV (not illustrated).

Membrane current noise. If a small change of light intensity is to be detected by a bipolar cell, then that intensity change must evoke a voltage in the bipolar cell that is larger than any noise in the bipolar cell's membrane potential produced by random opening and closing of ion channels in the cell membrane. The properties of this noise are expected to be different in isolated depolarizing and isolated hyperpolarizing bipolar cells because, in the absence of photoreceptor transmitter, the channels gated by this transmitter are expected to be closed in isolated hyperpolarizing cells and open in isolated depolarizing cells (Kaneko, 1971; Toyoda, 1973; Attwell et al., 1987). To rule out noise contributed by these photoreceptor transmitter–gated channels, we will concentrate on data from isolated hyperpolarizing cells (defined as cells showing an inward current at −50 mV in response to the putative photoreceptor transmitter glutamate [Attwell et al., 1987]). An analysis of the noise generated by the photoreceptor transmitter–gated channels and a comparison of the noise in isolated depolarizing and hyperpolarizing cells have been published elsewhere (Attwell et al., 1987).

The membrane current of isolated bipolar cells became visibly noisier at potentials depolarized from −40 mV and also at potentials more negative than −60 mV. An example is shown in Fig. 6*A* (data from long polarizations to different potentials). The increases in noise at depolarized and hyperpolarized potentials were seen consistently in >200 cells. Only when the seal obtained in the cell-attached recording mode was of low resistance and noisy was this voltage-dependent noise not detectable.

The spectral density of current fluctuations was greater at all frequencies when the cell was held at −75, −34, or −4 mV than when it was held at −53 mV, as shown in Fig. 6*C* (filled circles). However, an increased high-frequency (>10 Hz)

component contributed more to the noise increase at −4 than at −75 mV. The ion-substitution experiments described below showed that, at depolarized potentials, a large part of the increased noise positive to −30 mV was produced by outward K^+ current. Some of the noise increase at potentials below −70 mV was associated with large, channel-like, discrete jumps in membrane current (as near the start of the trace for −75 mV in Fig. 6*A*, and for the most negative pulse in Fig. 5), which were routinely observed in all cells. Thus, the noise increase at negative potentials is probably produced by a mechanism different from the noise increase at positive potentials.

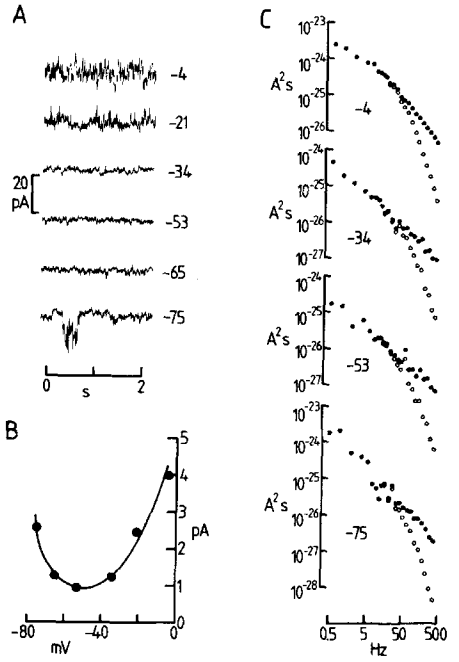

FIGURE 6. Membrane current noise in an isolated bipolar cell. (*A*) Specimen current records at different potentials (shown by each trace). (*B*) Standard deviation of the current noise in the frequency range 0–400 Hz, after (digital) filtering of the noise spectral density in *C* with the function $1/[1 + (2\pi\tau_m f)^2]$, plotted as a function of membrane potential. (τ_m was taken as 2.7 ms, as found for slice bipolar cells for *V* less than −25 mV. At −4 mV, the lower membrane resistance [Fig. 11] would make τ_m smaller, so that the standard deviation of the filtered current would be underestimated.) (*C*) Spectral density (in amperes squared times seconds) of the current noise (from traces like those in *A*) as a function of frequency (filled circles). The open circles show the same spectra multiplied by the function $1/[1 + (2\pi\tau_m f)^2]$ as described in the text. Instrumental noise was negligible. For this cell, the half-power frequency of filtering by the membrane capacitance and series resistance in the patch pipette was 900 Hz. Solution E of Table II was in the pipette.

In seven cells, the current variance (in the range 0–400 Hz) at −50 mV (i.e., at the minimum of the voltage-dependent noise and near the physiological dark potential) was 1.19 ± 0.56 pA^2.

The contribution of nonsynaptic current to bipolar cell voltage noise. When bipolar cells are not voltage-clamped, the current fluctuations like those in Fig. 6 will produce fluctuations in the cells' membrane potential, with a magnitude determined by the membrane resistance (discussed below). In addition, in the conversion of membrane current to membrane voltage, the fluctuations are filtered by the parallel combination of the membrane resistance, R_m, and capacitance, C_m. The effect of this low-pass filter is to reduce the effect of current variance at frequency f by a factor $1 + (2\pi\tau_m f)^2$, where τ_m is the membrane

constant ($\tau_m = R_m C_m$). To mimic the effect of this filtering, we first divided the spectra in Fig. 6*C* by this factor, using τ_m = 2.7 ms, a typical value for the membrane time constant of bipolar cells in retinal slices for voltages below about −25 mV (see below). The result is shown by the open circles in Fig. 6*C*. The standard deviation of the current fluctuations after such filtering is given by the square root of the area under the resulting spectra (Bendat and Piersol, 1971). This is plotted in Fig. 6*B*, where it is clear that the current noise reaches a minimum around −50 mV. The exact position of the current noise minimum varied somewhat between cells, but was usually between −40 and −60 mV.

The standard deviation we predict for the voltage fluctuations produced by the current noise in Fig. 6*A* is the product of the values shown in Fig. 6*B* and the membrane resistance, R_m. For slice bipolar cells, as described below, the mean input resistance we obtained in the physiological response range was 120 MΩ, i.e., roughly 10 times lower than for isolated cells. If this lower resistance is due to a synaptic conductance not present in isolated cells (and whose noise contribution is not considered in this calculation), then the standard deviation of the voltage noise predicted at −50 mV for the cell of Fig. 6 is obtained by multiplying the standard deviation of the filtered current fluctuations at −50 mV in Fig. 6*C* by 120 MΩ. The result is 115 μV (mean value, 106 ± 30 μV in seven cells). If, on the other hand, the higher input resistance for isolated bipolar cells reflects a loss of cell processes during the isolation procedure and the missing membrane contributes current noise with the same properties as that characterized in Fig. 6, then the standard deviation of the voltage noise produced in a bipolar cell in the retina would be larger than the figure of 115 μV calculated above by a factor of ~3 (the square root of the ratio of input resistances of isolated and slice bipolar cells). Thus, in the intact retina, the voltage noise generated by ion channels (other than those opened by the synaptic transmitters) is predicted to have a standard deviation of 100–300 μV. This noise may hinder the detection of dim stimuli (see Discussion).

Ion-Substitution Experiments

The experiments described in this section were performed to characterize in more detail the membrane currents in isolated bipolar cells.

Membrane currents with a raised external K^+ concentration. The effects of a raised external K^+ concentration ($[K^+]_o$) on the bipolar membrane currents were investigated for two reasons. First, we wished to test whether the time-dependent current seen on depolarization is carried by K ions. Second, when the retina is illuminated, $[K^+]_o$ in the inner retina initially increases (Kline et al., 1978), and it has been suggested that this reduces the sensitivity of the retina and thus contributes to light adaptation (Dowling and Ripps, 1976).

We studied cells bathed in external solution containing 15, 50, or 89.5 mM KCl (substituted for NaCl as listed in Table I), usually after recording the currents in the standard 1.5 mM $[K^+]_o$ solution, although some cells were studied solely in high-K^+ solution. An increase of $[K^+]_o$ depolarized the cells (Fig. 7*A*) and decreased their membrane resistance (Fig. 7*B*). The decrease in resistance may in principle contribute slightly to the decreased sensitivity of the retina

reported by Dowling and Ripps (1976) for high-K^+ solutions. However, since increasing $[K^+]_o$ from 1.5 to 89.5 mM only reduces the resistance by a factor of 3, while light increases $[K^+]_o$ in the proximal retina by <20%, this effect cannot account for a significant fraction of the reduction in sensitivity.

For 50 and 89.5 mM $[K^+]_o$, the Nernst potential for K ions (−17 and −2.8 mV, respectively, for 100 mM $[K^+]_i$) is in the range where the time-dependent

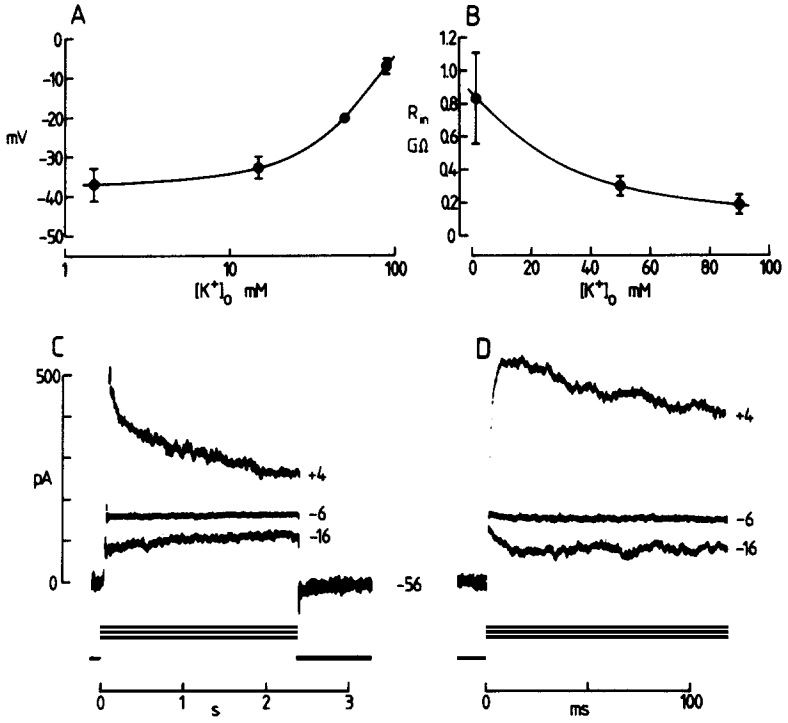

FIGURE 7. Effect of raising $[K^+]_o$ on the membrane currents. (*A*) Resting potentials (means ± SE) of cells in 89.5 (7 cells), 50 (3 cells), 15 (4 cells), and 1.5 (11 cells) mM $[K^+]_o$ solution. The curve, drawn by eye through the points, has a slope of 51 mV per decade change of $[K^+]_o$ at high $[K^+]_o$ and an average slope of 4 mV per decade between 1.5 and 15 mM $[K^+]_o$. (*B*) Input resistance at −50 mV as a function of $[K^+]_o$. (Membrane resistance was not studied for 15 mM $[K^+]_o$.) (*C* and *D*) Currents seen on depolarizing from a holding potential of −56 mV in 89.5 mM $[K^+]_o$, on a slow (*C*) and a fast (*D*) time base. Below the reversal potential for K ions, both the activation and inactivation phases of the time-dependent current are inverted. Solution C of Table II was in the pipette.

current is activated and then inactivated by depolarization. We would predict that, if the time-dependent current is carried by K ions, depolarization above the Nernst potential would evoke a rapid increase followed by a slow decrease in outward current as in 1.5 mM $[K^+]_o$ solution, but that depolarizing steps below the Nernst potential should evoke, after an instantaneous jump, a fast decrease followed by a slow increase in outward current. At the Nernst potential, there should be no time-dependent current. This is indeed how the time-dependent current behaved in 50 and 89.5 mM $[K^+]_o$ solution. An example for 89.5 mM

$[K^+]_o$ is shown in Fig. 7, *C* and *D*. The potentials at which there was no time-dependent change in current on depolarization were, on average, −20.0 ± 1.0 mV for three cells in 50 mM $[K^+]_o$ and −3.8 ± 5.0 mV for four cells in 89.5 mM $[K^+]_o$, reasonably close to the Nernst potentials quoted above.

A consistent feature of the data obtained in high-K^+ solution was that the potential at which the membrane current noise was minimal (see preceding section) was displaced to more positive potentials. For example, in Fig. 7*C*, the noise is at a minimum near −6 mV, rather than near −40 to −60 mV as in 1.5 mM $[K^+]_o$. It appears, therefore, that a significant fraction of the membrane current noise at positive potentials is generated by K^+ channels. At potentials

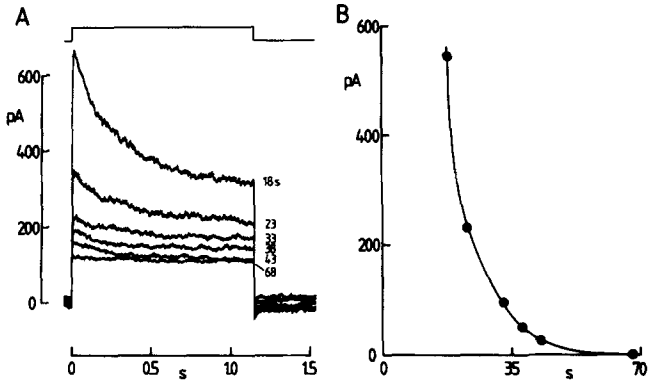

FIGURE 8. Removal of the time-dependent current by replacing internal K^+ with choline ions. The patch pipette contained solution I of Table II. (*A*) Membrane currents evoked on changing the pipette potential (top trace) from −45 to +31 mV, at various times (given by each trace) after going to the whole-cell recording configuration. (*B*) Amplitude of the peak time-dependent current (peak outward current minus instantaneous current jump seen on depolarization) as a function of time after going to whole-cell recording (abscissa). As choline enters and K^+ leaves the cells, the current decays to zero over a period of 1 min. The curve through the points, drawn by eye, approximates an exponential with a time constant of 8.5 s. The pipette series resistance for this cell was 13 MΩ.

below −10 mV, some of this noise may be generated by the time-dependent K^+ current described above. Above −10 mV, where that current is inactivated, the noise may be generated by other (time-independent) K^+ channels.

Membrane currents with no internal K^+. Cells studied with patch pipettes containing solution H or I from Table II, in which the K^+ had been replaced by Cs^+ (not illustrated) or choline (Fig. 8), showed a characteristic decline in their outward-gated current during the first minute after going to the whole-cell recording configuration. Over the same period, the resting potential depolarized to ~0 mV. This behavior is attributed to the impermeant cations in the pipette exchanging with the K ions in the cell (cf. Kaneko and Tachibana, 1985; Lewis and Hudspeth, 1983). After this decline of the time-dependent current, the membrane current-voltage relation was approximately linear and time independent.

Membrane currents with 10 and 100 mM $[Cl^-]_i$ solution. The membrane ionic currents recorded when the patch pipette contained 10 or 100 mM $[Cl^-]_i$ solution

(solution A or D in Table II) were not detectably different from those seen with 30 mM $[Cl^-]_i$ solution. Negative to −30 mV, the membrane current was time independent, and for depolarizing steps past −30 mV, a rapid increase of outward current followed by a slow decrease in outward current was seen. At −50 mV, the input resistance was 1.03 ± 0.86 GΩ (n = 24) for 10 mM $[Cl^-]_i$ and 0.99 ± 0.93 GΩ (n = 56) for 100 mM $[Cl^-]_i$, i.e., not significantly different from the value for 30 mM $[Cl^-]_i$. The mean resting potentials for 10 mM $[Cl^-]_i$ (−46.6 ± 15.6 mV, uncorrected for shunting by the seal conductance) and 100 mM $[Cl^-]_i$ (−38.2 ± 16.1 mV) were also essentially the same as those obtained with 30 mM $[Cl^-]_i$.

We conclude, therefore, that neither the time-independent currents below −30 mV nor the time-dependent currents above −30 mV are carried to a large extent by Cl ions (or, less likely, that the acetate that we substituted for Cl can pass through the ion channels just as well as Cl).

Membrane currents with different internal Ca^{2+} buffering. The membrane currents shown in Fig. 3 were obtained using patch pipette solutions containing 0.6 mM EGTA and 17.5 μM Ca^{2+} and were calculated to have a free $[Ca^{2+}]$ of 1.1×10^{-8} M. To test the possibility that the time-dependent outward current is activated by a rise in $[Ca^{2+}]_i$ after depolarization, we carried out experiments using patch pipette solutions providing a wide range of $[Ca^{2+}]_i$ values and buffering powers.

A lower buffering power than that of our standard solution was provided by solution E of Table II, which contained only 20 μM EGTA (and 17.5 μM Ca^{2+}) and was calculated to have a free $[Ca^{2+}]$ of 1.5 μM. In 40 cells studied with this pipette solution, the membrane currents were not significantly different from those found with 0.6 mM EGTA in the pipette solution (Fig. 9*A*). The mean input resistance at −50 mV was 1.2 ± 1.4 GΩ (cf. 1.3 ± 2.2 GΩ for cells with 0.6 mM EGTA), and the time-dependent outward current was, on average, no larger in amplitude or faster in onset than with 0.6 mM EGTA in the pipette.

A higher buffering power was provided by pipette solutions containing 5 mM EGTA and 0.5 mM Ca^{2+} (solution F in Table II, with a free $[Ca^{2+}]$ of 4.2×10^{-8} M), or containing 87 mM KF, in addition to 5 mM EGTA and 0.5 mM Ca^{2+} (solution G, with a free $[Ca^{2+}]$ of $<5.2 \times 10^{-9}$ M: this solution should give better buffering of internal Ca^{2+} than 5 mM EGTA alone, because of the high $[F]_i$). Cells studied with these internal solutions had time-dependent currents with amplitudes and time courses that were not significantly different (Fig. 9, *B* and *C*) from those found with 0.6 mM or 20 μM EGTA in the patch pipette (cf. Cahalan et al., 1985).

Currents with no external Ca^{2+}. Further evidence that an inward Ca^{2+} current, raising $[Ca^{2+}]_i$, is not needed to activate the outward time-dependent current was provided by experiments in which cells were superfused with a solution in which the Ca^{2+} in the normal external solution was replaced by Mg^{2+} and 0.2 mM EGTA was added ("zero-Ca" solution in Table I). The free $[Ca^{2+}]$ calculated for this solution was 1.1×10^{-8} M, low enough for the electrochemical gradient for Ca^{2+} to be outward at potentials >0 mV.

Application of this solution did not abolish the time-dependent current (Fig.

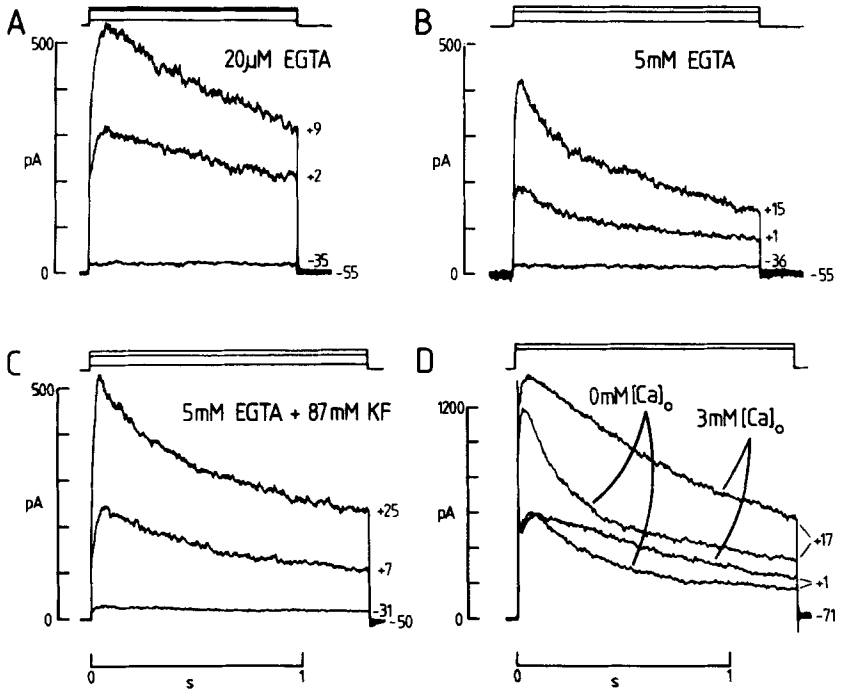

FIGURE 9. The time-dependent current is not activated by a rise of $[Ca^{2+}]_i$. (*A–C*) Data from three different cells studied with different $[Ca^{2+}]_i$ and buffering power. (*A*) Patch pipette containing 20 μM EGTA (solution E), giving free $[Ca^{2+}]_i$ = 1.5 μM with minimal $[Ca^{2+}]$ buffering. (*B*) Pipette containing 5 mM EGTA (solution F), giving $[Ca^{2+}]_i = 4.2 \times 10^{-8}$ M with more Ca^{2+} buffering than for part *A* or for Fig. 3. (*C*) Pipette containing 5 mM EGTA and 87 mM KF (solution G), giving $[Ca^{2+}]_i < 5.2$ nM and strong Ca^{2+} buffering. The membrane potential during depolarization is given next to each trace. Contrary to what would be expected if the time-dependent current were Ca^{2+}-gated, the current was not significantly smaller or slower in onset when studied with solutions of a higher Ca^{2+} buffering power inside the cell. The cell-to-cell variations of the time course of the gated current seen in the cells are no greater than are observed between different cells, all studied with the same pipette solution. (*D*) Removal of $[Ca^{2+}]_o$ does not abolish the gated current. After recording the response to depolarization in normal solution (3 mM $[Ca^{2+}]_o$), the cell was superfused with solution containing 0.2 mM EGTA and no added Ca^{2+}. The change in the kinetics of the current is probably due to the surface potential of the membrane being altered on removing Ca^{2+}.

9*D*). Indeed, the current remained of approximately the same amplitude although its inactivation kinetics were speeded, probably because of a change in the membrane surface potential in the absence of Ca^{2+} (although we substituted Mg^{2+} for Ca^{2+} to minimize such effects).

These results suggest that the majority of the time-dependent current is not Ca^{2+}-gated and therefore is presumably voltage-gated. A similar approach has been employed by Cahalan et al. (1985) to show that a time-dependent K^+ current in T lymphocytes is not Ca^{2+}-gated.

Cells in Retinal Slices

Bipolar cells, identified as described in the Methods, were patch-clamped in situ in slices of retina. We considered these experiments crucial, because they allowed us to compare the membrane properties of isolated bipolar cells with those of cells in the retina.

Out of 84 cells recorded from, 8 cells were positively identified as depolarizing bipolar cells. No cells were unambiguously identified as hyperpolarizing bipolar cells. This low success rate reflects the difficulty of patch-clamping in retinal slices, where debris on the slice surface often hinders gigaseal formation, and of identifying hyperpolarizing bipolar cells, which can be confused with horizontal cells (which also hyperpolarize in response to light).

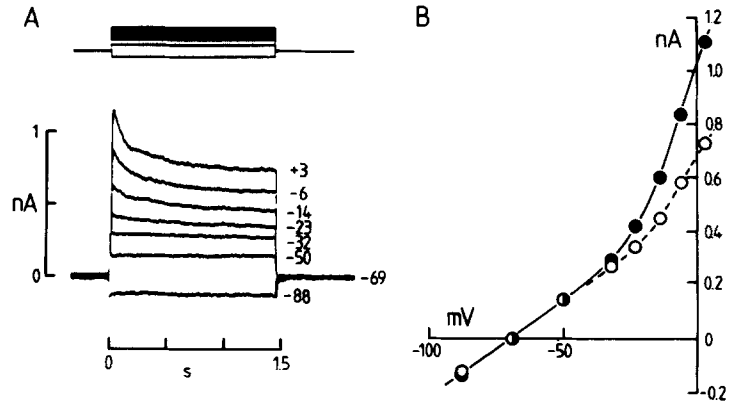

FIGURE 10. (*A*) Ionic currents in a depolarizing bipolar cell in the retinal slice. The voltage-clamp potentials are shown next to each trace. (*B*) Plots of the membrane current-voltage relations at the peak of the current in *A* (filled circles) and in the steady state (open circles). Solution A of Table II was in the pipette.

Resting potential, capacitance, and input resistance. Depolarizing bipolar cells had resting potentials ranging from −80 to −14 mV (uncorrected for seal resistance) with a mean value of −28 ± 22 mV. The membrane capacitance, obtained from the current response to a small voltage-clamp pulse applied from a holding potential of −50 mV, was 21.4 ± 11.0 pF. The current-voltage relation of slice bipolar cells was roughly ohmic below −40 mV (Fig. 10*A*). The measured input resistances in this voltage range were between 63 and 300 MΩ (mean, 120 ± 80 MΩ), and the mean membrane time constant was 2.7 ms.

Voltage-gated currents. In four of the eight depolarizing bipolar cells studied, depolarization past −30 mV evoked a fast time-dependent increase in outward current followed by a slow time-dependent decrease in outward current (Fig. 10*A*), as for isolated cells. As a consequence, the steady state current-voltage relation showed less rectification than that measured at the peak of the outward current (Fig. 10*B*). The other four depolarizing bipolar cells showed time-independent responses to voltage-clamp steps between −80 and +20 mV, with mild outward rectification above −20 mV.

Membrane current noise. As for isolated bipolar cells, the noise in the membrane current of slice bipolar cells was voltage dependent, with a minimum around −40 to −60 mV (Fig. 11*A*). The noise spectra of data like those in Fig. 11*A* are shown in Fig. 11*C*. The open symbols in this figure show the effect of filtering the raw spectra to mimic the effect of filtering by the membrane time constant in the conversion of membrane current to membrane voltage (as done for the isolated cell data in Fig. 6*C*). In Fig. 11*B*, the standard deviation of the filtered fluctuations is shown as a function of voltage. The value of voltage noise predicted for the minimum standard deviation of 1.5 pA in Fig. 11*B* is 180 μV (obtained by multiplying the current noise by the mean input resistance for slice bipolar cells of 120 MΩ). In four cells, the average value of the minimum voltage noise thus calculated was 239 ± 104 μV.

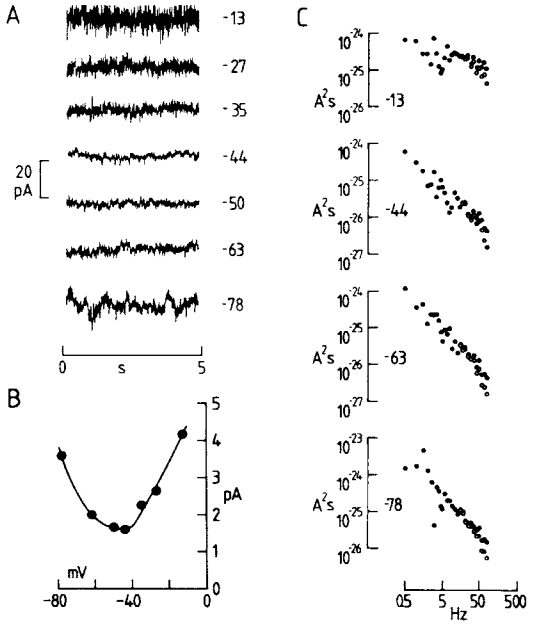

FIGURE 11. Membrane current noise in a depolarizing bipolar cell in a retinal slice. (*A*) Specimen current records at different potentials (shown next to each trace). (*B*) Standard deviation of the current noise in the frequency range 0–500 Hz, obtained after digital filtering of the noise spectral density in *C* with the function $1/[1 + (2\pi\tau_m f)^2]$, where τ_m = 2.7 ms, plotted as a function of membrane potential. As for Fig. 6*B*, the use of the value of τ_m appropriate to *V* less than −25 mV will result in the point at −13 mV being an underestimate of the filtered fluctuations. (*C*) Spectral density of the current noise (from traces like those in *A*; the membrane potential given next to each graph), as a function of frequency (filled circles). The open circles show the same spectra multiplied by the function $1/[1 + (2\pi\tau_m f)^2]$. For this cell, the half-power frequency of filtering by the membrane capacitance and series resistance in the patch pipette was 160 Hz. Solution E was in the pipette.

DISCUSSION

The Importance of Bipolar Membrane Currents for Visual Signal Processing

Bipolar cells serve as a key relay between the outer retina, where light is converted into an electrical signal by photoreceptors, and the inner retina, where visual information is coded into action potentials for transmission along the optic nerve. Visual information can be processed in the bipolar cell layer either as a result of the pattern of synaptic convergence onto the cells (e.g., generating center-surround receptive fields) or as a result of shaping by currents intrinsic to the

bipolar cell membrane (e.g., enhancing the transience of the signal so that more emphasis is given to illumination changes, such as occurs in photoreceptors [Attwell and Wilson, 1980]). In this article, we have concentrated on the latter aspect of bipolar cell function, investigating the role of nonsynaptic membrane currents in shaping the light response and in setting the level of voltage noise in bipolar cells. As discussed in detail below, our results show that axolotl bipolar cells process visual information in a way different from goldfish bipolar cells, and show that nonsynaptic currents generate significant noise in the membrane potential.

Ionic Currents in Axolotl Bipolar Cells

The bipolar membrane current-voltage relation is approximately ohmic between −30 and −70 mV. At potentials above −30 mV, the membrane exhibits outward rectification: outward current, carried largely by K ions, flows through voltage-gated channels, which are initially opened and then inactivated on depolarization. We have not carried out a full kinetic analysis of this current because its voltage range of activation is largely outside the physiological range: the resting potential of bipolar cells in the dark is typically around −45 mV and light can depolarize or hyperpolarize the two classes of cells by up to 25 mV (Simon et al., 1975; Lasansky, 1978; Ashmore and Falk, 1980, 1982; Ashmore and Copenhagen, 1983; Saito and Kaneko, 1983; Borges, S., and M. Wilson, unpublished observations on axolotl bipolar cells).

It is surprising that the ionic currents present in axolotl bipolar cells differ in several important respects from those in goldfish bipolar cells (Kaneko and Tachibana, 1985). Kaneko and Tachibana (1985) describe two outward currents thought to be carried by K ions. One of these is voltage-gated and roughly resembles the outward K^+ current reported here in that it is both activated and inactivated by depolarization, but it differs from the current in axolotl cells in having much slower kinetics. A second K^+ current described by Kaneko and Tachibana (1985) is believed, from several lines of evidence, to be gated by Ca ions. A large Ca^{2+}-gated current in axolotl bipolar cells is ruled out by our results with removal of external Ca^{2+} and with altered internal Ca^{2+} buffering (cf. Cahalan et al., 1985).

Shaping of the Voltage Response to Light

A further difference between the currents of goldfish bipolar cells and those of axolotl is the presence in goldfish of an inward time-dependent current activated by hyperpolarization. Functionally, this difference is the most significant. In goldfish, the inward current, which is activated in the physiological potential range, is likely to be significant in shaping the light responses of these cells, making the voltage responses more transient than the synaptic current. In axolotl bipolar cells, however, the ohmic response to voltage steps between −30 and −70 mV implies that in this potential range the waveform of the bipolar voltage response to light will be determined by the waveform of the synaptic current injected into the cell from photoreceptors and from other cells (apart from a small amount of filtering by the membrane capacitance). This absence of a voltage-gated current enhancing transience in axolotl bipolar cells is interesting

in view of Marr and Ullman's (1981) suggestion that transience in the response of cells with a center-surround receptive field plays a crucial role in movement detection.

The transient outward current in axolotl bipolar cells, which is rapidly activated and slowly inactivated by depolarization, may shape the bipolar cells' light response at the most depolarized end of its response range—for example, at the onset of the response to bright light in depolarizing bipolar cells and during the rapid depolarization produced in hyperpolarizing bipolar cells when light is removed.

Comparison of Isolated Bipolar Cells with Those in Retinal Slices

The resistance of bipolar cells in retinal slices is ~10 times lower than that of isolated bipolar cells, presumably because of synaptic input from other retinal neurons and electrical coupling of bipolar cells (Wong-Riley, 1974; Kujiraoka and Saito, 1986), and because the isolation procedure results in a loss of some cell processes. The voltage-gated currents of bipolar cells in retinal slices are broadly similar to those of isolated cells (compare Figs. 3 and 10). This similarity supports the view that our isolation procedure does not selectively remove classes of ion channels from the cell membrane. It could be argued that the use of whole-cell recording, by altering the intracellular medium, results in the loss of functionally relevant currents, both in slices and in isolated cells. We consider this unlikely, however: in rods, where both whole-cell and conventional two-microelectrode voltage-clamping have been used to study membrane currents shaping the light response, similar results have been obtained (Attwell and Wilson, 1980; Bader and Bertrand, 1984).

Noise

For dim stimuli to be detected by bipolar cells, they must produce a voltage change in the bipolar cell that is at least comparable to the noise in the bipolar cell's membrane potential. The membrane potential is noisy because of fluctuations in membrane currents intrinsic to the bipolar cell and fluctuations in currents evoked by synaptic transmitters released from other cells. In this article, we have shown (Fig. 6) that the membrane current noise produced by nonsynaptic ion channels is voltage dependent, with a minimum at around −40 to −60 mV. The location of this minimum, close to the dark potentials of bipolar cells in the intact retina (Miller and Dacheux, 1976; Wu, 1985), suggests that the nonsynaptic membrane currents have become optimized, through evolution, to facilitate detection of weak stimuli.

The membrane current fluctuations occur over a wide frequency range (Fig. 6*C*). If stimuli are detected (at a level of the visual system after the bipolar cells) by simply determining whether the signal reaches a certain threshold amplitude or not, then noise at all frequencies up to those where filtering by the membrane capacitance occurs will hinder the detection of weak stimuli. On this basis, we calculate (Fig. 6*B*) that the voltage noise owing to nonsynaptic channels will have a standard deviation of ~100–300 μV. For comparison, a 250-μV voltage change is produced by a single photon in dogfish bipolar cells (Ashmore and Falk, 1982), and in the *Ambystoma* retina, absorption of one photon by each of the 1,000 rods

in the bipolar receptive field center generates a response of 600–900 μV (Hare et al., 1986, Fig. 1). It is possible, however, that something akin to matched filtering occurs after the bipolar cells, so that noise at frequencies above those of the light-evoked signal is irrelevant because it is filtered out, enhancing the signal-to-noise ratio. Even in this case, consideration of the noise spectra in Fig. 6*C* shows that the noise in the frequency range of the light response still exhibits a minimum around −40 to −60 mV. In axolotl bipolar cells, the signal evoked by dim light has power at frequencies below ~10 Hz (Borges, S., and M. Wilson, unpublished observations), similar to the situation in turtle, dogfish, and tiger salamander bipolar cells (Ashmore and Copenhagen, 1980; Ashmore and Falk, 1982; Hare et al., 1986).

The membrane current of depolarizing bipolar cells in the unilluminated retinal slice also shows voltage-dependent noise with a minimum around −40 to −60 mV (Fig. 11). Its standard deviation at the minimum is ~2.5 times that observed in isolated cells. The larger noise in slice cells is due partly to any intrinsic channels present in cell processes that are lost during the cell isolation procedure, and partly to synaptic conductance not present in the isolated cells. This voltage-dependent noise complicates the interpretation of results (Simon et al., 1975; Ashmore and Falk, 1982) showing that light alters voltage noise in bipolar cells, since some of the noise alteration will have occurred because of the light-induced change in membrane potential.

We thank Stuart Bevan for help with early retinal dissociations, Walter Stewart for a gift of Lucifer yellow, David Colquhoun and Armand Cachelin for computer facilities and advice, Karl Swann and John Kentish for computer programs, Lindsey Alldritt for secretarial assistance, and Jerry Lockett for photographic services.

This work was supported by grants from the Medical Research Council, the Wellcome Trust, the Nuffield Foundation, Fight for Sight (U.K.), NATO (Collaborative Research Grant RG.85/0471), the Central Research Fund of London University, the National Institutes of Health (EY-04112 to M. Wilson), the British Council (to M. Tessier-Lavigne), and the Royal Society (to D. Attwell).

Original version received 10 October 1986 and accepted version received 10 August 1987.

REFERENCES

Aldrich, R. W., P. A. Getting, and S. H. Thompson. 1979. Inactivation of delayed outward current in molluscan neuronal somata. *Journal of Physiology.* 291:507–530.

Ashmore, J. F., and D. R. Copenhagen. 1980. Different postsynaptic events in two types of retinal bipolar cell. *Nature.* 288:84–86.

Ashmore, J. F., and D. R. Copenhagen. 1983. An analysis of transmission from cones to hyperpolarizing bipolar cells in the retina of the turtle. *Journal of Physiology.* 340:569–597.

Ashmore, J. F., and G. Falk. 1980. Responses of rod bipolar cells in the dark-adapted retina of the dogfish, *Scyliorhinus canicula. Journal of Physiology.* 300:115–150.

Ashmore, J. F., and G. Falk. 1982. An analysis of voltage noise in rod bipolar cells of the dogfish retina. *Journal of Physiology.* 332:273–297.

Attwell, D., S. Bevan, P. Mobbs, M. Tessier-Lavigne, and M. Wilson. 1985*a*. Membrane currents in bipolar cells isolated from the axolotl retina, recorded by whole-cell patch-clamping. *Journal of Physiology.* 360:19P. (Abstr.)

Attwell, D., P. Mobbs, M. Tessier-Lavigne, and M. Wilson. 1985*b*. Membrane currents in depolarizing bipolar cells recorded by whole-cell patch-clamping in living retinal slices from the axolotl retina. *Journal of Physiology.* 365:34P. (Abstr.)

Attwell, D., P. Mobbs, M. Tessier-Lavigne, and M. Wilson. 1986. Noise changes associated with the action of glutamate on retinal bipolar cells of the salamander (*Ambystoma mexicanum*). *Journal of Physiology.* 371:39P. (Abstr.)

Attwell, D., P. Mobbs, M. Tessier-Lavigne, and M. Wilson. 1987. Neurotransmitter-induced currents in retinal bipolar cells of the axolotl, *Ambystoma mexicanum. Journal of Physiology.* 387:125–161.

Attwell, D., F. S. Werblin, and M. Wilson. 1982. The properties of single cones isolated from the tiger salamander retina. *Journal of Physiology.* 328:259–283.

Attwell, D., and M. Wilson. 1980. Behaviour of the rod network in the tiger salamander retina mediated by membrane properties of individual rods. *Journal of Physiology.* 309:287–315.

Bader, C. R., and D. Bertrand. 1984. Effect of changes in intra- and extracellular sodium on the inward (anomalous) rectification in salamander photoreceptors. *Journal of Physiology.* 347:611–631.

Bader, C. R., P. R. Macleish, and E. A. Schwartz. 1979. A voltage-clamp study of the light response in solitary rods of the turtle. *Journal of Physiology.* 296:1–26.

Baylor, D. A., G. Matthews, and B. J. Nunn. 1984. Location and function of voltage-sensitive conductances in retinal rods of the salamander, *Ambystoma tigrinum. Journal of Physiology.* 354:203–223.

Baylor, D. A., and B. J. Nunn. 1986. Electrical properties of the light-sensitive conductance of rods of the salamander, *Ambystoma tigrinum. Journal of Physiology.* 371:115–145.

Bendat, J. S., and A. G. Piersol. 1971. Random Data. Wiley-Interscience, New York. 407 pp.

Cajal, S. R. 1893. La retine des vertebres. *La Cellule.* 9:17–257.

Cahalan, M. D., K. G. Chandy, T. E. DeCoursey, and S. Gupta. 1985. A voltage-gated K^+ channel in human T lymphocytes. *Journal of Physiology.* 358:197–237.

Connor, J. A., and C. F. Stevens. 1971*a*. Inward and delayed outward membrane currents in isolated neural somata under voltage clamp. *Journal of Physiology.* 213:1–19.

Connor, J. A., and C. F. Stevens. 1971*b*. Voltage clamp studies of a transient outward current in gastropod neural somata. *Journal of Physiology.* 213:21–30.

Detwiler, P. B., A. L. Hodgkin, and P. A. McNaughton. 1978. A surprising property of electrical spread in the network of rods in the turtle's retina. *Nature.* 274:562–565.

Dowling, J. E., and H. Ripps. 1976. Potassium and retinal sensitivity. *Brain Research.* 107:617–622.

Falk, G., and P. Fatt. 1974. Limitations to single photon sensitivity in vision. *In* Lecture Notes in Biomathematics. Vol. 4: Physics and Mathematics of the Nervous System. M. Conrad, W. Güttinger, and M. Dal Cin, editors. Springer-Verlag, Berlin. 171–204.

Fenwick, E. M., A. Marty, and E. Neher. 1982. A patch-clamp study of bovine chromaffin cells and of their sensitivity to acetylcholine. *Journal of Physiology.* 331:577–597.

Fukushima, Y., S. Hagiwara, and M. Henkart. 1984. Potassium current in clonal cytotoxic T lymphocytes. *Journal of Physiology.* 351:645–656.

Goldman, D. E. 1943. Potential, impedance and rectification in membranes. *Journal of General Physiology.* 27:37–60.

Hamill, O. P., A. Marty, E. Neher, B. Sakmann, and F. J. Sigworth. 1981. Improved patch-clamp techniques for recording from cells and cell-free membrane patches. *Pflügers Archiv.* 391:85–100.

Hare, W. A., J. S. Lowe, and G. Owen. 1986. Morphology of physiologically identified bipolar

cells in the retina of the tiger salamander, *Ambystoma tigrinum*. *Journal of Comparative Neurology*. 252:130–138.

Hodgkin, A. L., and A. F. Huxley. 1952*a*. Currents carried by sodium and potassium ions through the membrane of the giant axon of *Loligo*. *Journal of Physiology*. 116:449–472.

Hodgkin, A. L., and A. F. Huxley. 1952*b*. The dual effect of membrane potential on sodium conductance in the giant axon of *Loligo*. *Journal of Physiology*. 116:497–506.

Kaneko, A. 1971. Physiological studies of single retinal cells and their morphological identification. *Vision Research*. 3(Suppl.):17–26.

Kaneko, A., and M. Tachibana. 1985. A voltage-clamp analysis of membrane currents in solitary bipolar cells dissociated from *Carassius auratus*. *Journal of Physiology*. 358:131–152.

Kline, R. P., H. Ripps, and J. E. Dowling. 1978. Generation of b-wave currents in the skate retina. *Proceedings of the National Academy of Sciences*. 75:5727–5731.

Kujiraoka, T., and T. Saito. 1986. Electrical coupling between bipolar cells in carp retina. *Proceedings of the National Academy of Sciences*. 83:4063–4066.

Landolt, E. 1871. Beiträge zur Anatomie der Retina von Frosch, Salamander und Triton. *Archiv für Mikroskopie und Anatomie*. 7:81–100.

Lasansky, A. 1973. Organization of the outer synaptic layer in the retina of the larval tiger salamander. *Proceedings of the Royal Society of London, Series B*. 265:471–489.

Lasansky, A. 1978. Contacts between receptors and electrophysiologically identified neurones in the retina of the larval tiger salamander. *Journal of Physiology*. 285:531–542.

Lewis, R. S., and A. J. Hudspeth. 1983. Voltage- and ion-dependent conductances in solitary vertebrate hair cells. *Nature*. 304:538–541.

Marr, D., and S. Ullmann. 1981. Directional sensitivity and its use in early visual processing. *Proceedings of the Royal Society of London, Series B*. 211:151–180.

Marty, A., and E. Neher. 1983. Tight-seal whole-cell recording. *In* Single Channel Recording. B. Sakmann and E. Neher, editors. Plenum Publishing Corp., New York. 107–121.

Miller, R. F., and R. F. Dacheux. 1976. Synaptic organization and ionic basis of on and off channels in mudpuppy retina. III. A model of ganglion cell receptive field organization based on chloride-free experiments. *Journal of General Physiology*. 67:679–690.

Saito, T., and A. Kaneko. 1983. Ionic mechanisms underlying the responses of off-center bipolar cells in the carp retina. I. Studies on responses evoked by light. *Journal of General Physiology*. 81:589–601.

Schwartz, E. A. 1974. Responses of bipolar cells in the retina of the turtle. *Journal of Physiology*. 236:211–224.

Simon, E. J., T. D. Lamb, and A. L. Hodgkin. 1975. Spontaneous voltage fluctuations in retinal cones and bipolar cells. *Nature*. 256:661–662.

Smith, R. M., and A. E. Martell. 1976. Critical Stability Constants. Vol. 4: Inorganic Complexes. Plenum Publishing Corp., New York. 257 pp.

Toyoda, J.-I. 1973. Membrane resistance changes underlying the bipolar cell response in carp retina. *Vision Research*. 13:283–294.

Werblin, F. S. 1978. Transmission along and between rods in the tiger salamander retina. *Journal of Physiology*. 280:449–470.

Wong-Riley, M. T. T. 1974. Synaptic organization of the inner plexiform layer in the retina of the tiger salamander. *Journal of Neurocytology*. 3:1–33.

Wu, S. M. 1985. Synaptic transmission from rods to bipolar cells in the tiger salamander retina. *Proceedings of the National Academy of Sciences*. 82:3944–3947.